Jurnal Teknologi, 35(D) Dis. 2001: 1–14

CRITICAL REMARKS ON SOME APPLICATIONS OF DIGITAL IMAGE ANALYSIS WITH EMPHASIS ON STATISTICAL METHODOLOGY

OMAR MOHD. RIJAL[1], NORLIZA MOHD. NOOR[2] & CHANG YUN FAH[3]

Abstract. The results of Rijal and Noor [1] and [2] regarding the use of statistical methods and sources of uncertainty associated with making inferences when using digital images provide the motivation for this study. In this paper three other examples are presented with the purpose of providing an overview of applications (possibly statistical) of image analysis, and general issues highlighted. One conclusion from this study is that statistical/mathematical methodology should be emphasized in digital image analysis.

Keywords: Digital image analysis,

Abstrak. Hasil penyelidikan dari Rijal dan Noor [1] dan [2] mengenai kegunaan kaedah statistik dan punca ketidakpastian yang berhubungkait dengan membuat pentadbiran ketika menggunakan imej digit memberi motivasi kepada kajian ini. Dalam kertas kerja ini tiga contoh lagi dikemukakan dengan tujuan memberi pandangan keseluruhan mengenai applikasi (termasuk secara statistik) analisis imej digit, dan isu-isu am diberi penekanan. Satu kesimpulan dari kajian ini adalah kaedah statistik/ matematik harus diberi peranan penting dalam analisis imej digit.

Kata Kunci: Analisis imej digit, kaedah statistik, perbandingan secara kritikal contoh-contoh terpilih.

1.0 INTRODUCTION

Some problems with frequently used statistical methods in digital image analysis have been highlighted [1]. The use of the Binomial Markov Random Field (BMRF) to model texture resulted in a 'reasonable' segmentation of a particular Landsat image. This observation suggests the preference, amongst statistical methods, for neighbourhood based segmentation techniques.

The analysis of complex digital imagery demands that an overall assessment of the quality of decision be made. Rijal and Noor [2] regards the decision making process as being composed of two parts, viz:

1 Inst. of Mathematical Sc., Faculty of Science, University Malaya.
2 Electrical Eng. Course, Diploma Program, Universiti Teknologi, Malaysia.
E-mail: norliza@utmkl.utm.my
3 Faculty of Engineering, Multimedia University. E-mail: cyfah@yahoo.com

(i) the creation of the image and
(ii) interpretation of the image;

both of which create uncertainties. Problems associated with (ii) involve issues of visual/image perception and the use of misclassification probabilities.

In this paper, the role of statistical methodology in image analysis in the presence of the above mentioned uncertainties is investigated by studying three other applications of image analysis;

(i) diagnosis of Pulmonary Tuberculosis caused by the Mycobacterium Tubercle Bacilli (MTB) using chest X-ray films,
(ii) the Glaucoma disease, and
(iii) the recognition of symbols in utility maps.

The authors here define statistical methodology as the use of;

(A) Non-probabilistic approaches and ideas, such as graphical techniques. Methods or techniques related to the use of image histogram appear most popular.
(B) Probabilistic technique, where direct reference to a specific probability distribution is involved.

Inferences or conclusions from applying statistical methodology ideally makes use of an image model. The 'probabilistic' nature of image models usually depends on the nature and extent of dependency of a pixel intensity on intensities of its neighbours. In particular, the Markov Random Field Model has seen wide applications, see example Besag [3], [4], Cross and Jain [5], Ripley [6], and Derin and Elliot [7]. When the dependency of neighboring pixels may be justifiably ignored (usually a simpler type of image is being studied) fitting mixture distributions, see for example, Samadani [8], Noor *et al*. [9] and Sclove [10], or density estimation methods, see Duin [11], yields useful probability models of the image. When image models are difficult to derive, most of the image analysis centres around the difficult task of obtaining 'descriptors' or 'statistics', for example, Haralick and Shanmugam [12] discussed sixteen texture measures that can be used with the Gray Level Co-occurrence Matrix (GLCM). However, Haralick, Shanmugam and Dinstein [13] indicates that it is difficult to identify which specific textural characteristics are represented by each of these features. This is a typical problem with non-probabilistic approach.

2.0 THREE OTHER EXAMPLES OF THE APPLICATIONS OF IMAGE ANALYSIS

The following examples and the remote sensing problem in Rijal and Noor [2] would be sufficient to illustrate the key points. These examples were selected to show different sources of uncertainties when analysing digital images, and in particular how statistical methodology may help in the analysis.

Example 1: MTB

Historically, X-rays are extensively used (on its own or with other tests such as sputum tests); and also due to economic considerations the 'common' X-ray is still an important ingredient in the diagnostic process despite rapid advances in medical imaging technology (see Middlemiss [14] and Moores [15]). A description on the reliability of chest radiography is discussed in Toman [16], page 28. Although digital images for MTB patients may be directly obtained from sophisticated imaging system, such equipment is only available to particular medical centres simply due to cost considerations. As such, we acknowledge that problems and drawbacks exist in using digital images by scanning conventional X-ray films. Nevertheless, most of the district hospitals in Malaysia are equipped with conventional X-ray machine, plus the availability of affordable scanning devices make this study relevant.

On the X-ray film, the area affected by MTB appears as white spots or 'snow-flakes' due to a hardening of lung tissues. The greater the intensity of white spots the more serious is the disease. For the severe cases 'cavities' appear as a patch, low intensity white spots in the middle of a wide spread and higher intensity white spots. An immediate difficulty is that,

(i) The size, shape and position of white spots are totally random other than at the upper parts of the lungs (nearer to the throat) which tend to be affected first. In fact MTB is often mistaken for other lung ailments;
(ii) The experience of the particular medical practitioner may also be an important factor. Problems associated with visual interpretation are significant, where an illustration of this problem is discussed in pages 28-37 in Toman [16].

Figures 1, 2 and 3 (dated 22nd June, 29th June and 7th July 1987, respectively) show three chest X-rays of the same patient who is a confirmed MTB patient. Figure 1 shows a wide spread 'white area' (partly due to low resolution) and after about two weeks of medication. Figure 3 shows a considerable improvement (disappearance of some of the white area). A histogram of gray-levels for each X-ray were obtained and plotted simultaneously. Figure 1(b), Figure 2(b) and Figure 3(b) show a gradual increase in pixel frequency (around pixel value of 50) and a gradual decrease in pixel frequency

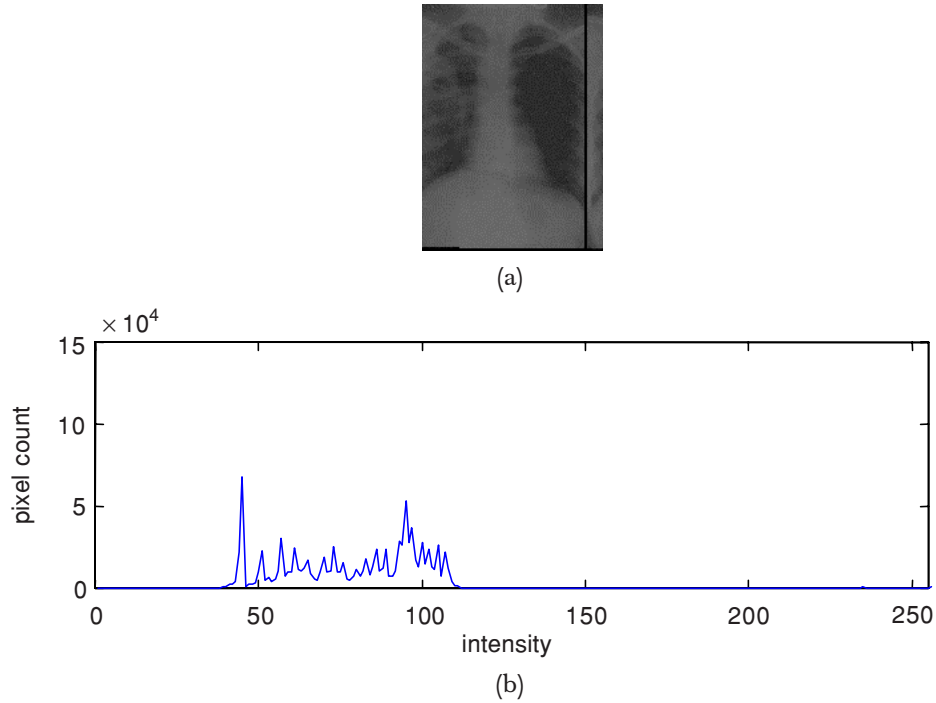

Figure 1 (a) A Chest X-ray Image of a Confirmed MTB Patient Dated 22nd June 1987. (b) Histogram of Image Figure 1(a)

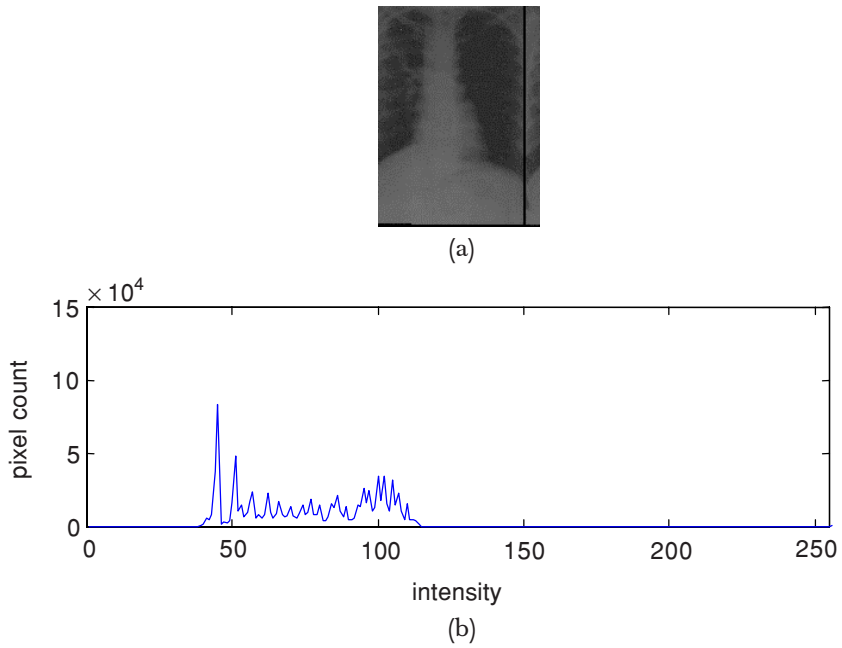

Figure 2: (a) A Chest X-ray Image dated 29th June 1987 of the Same MTB Patient after One Week of Medication. (b) Histogram of Image Figure 2(a)

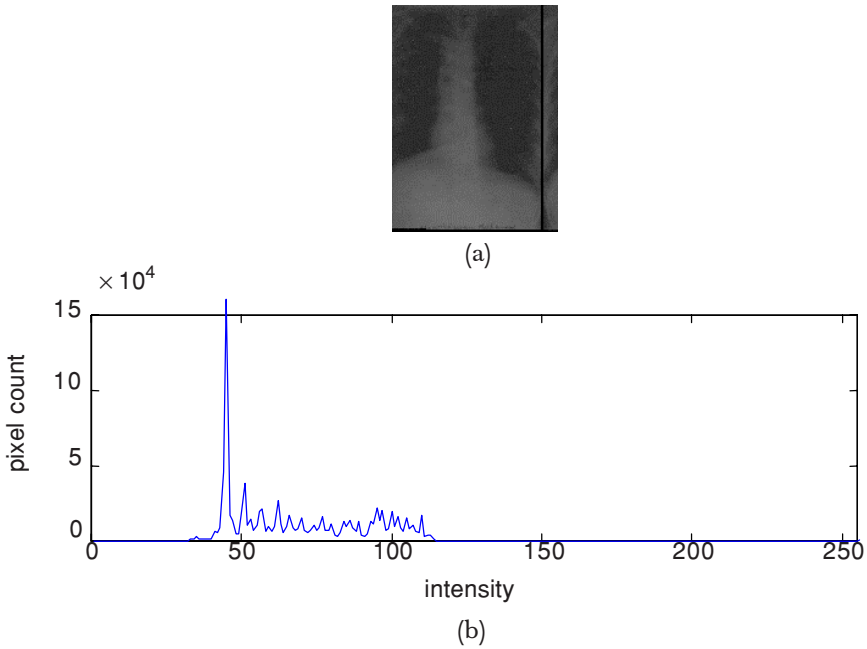

Figure 3 (a) A Chest X-ray Image Dated 7th July 1987 of the Same Patient after Two Weeks of Medication. (b) Histogram of Image (a)

(around pixel values 100). Although the shape of the histogram is not robust and may change easily, Silverman [17], this problem can be considerably reduced if the process of creating the images is carried out under consistent conditions. For example the same technician is assigned to a given patient.

The next logical step is some form of modeling based on the histograms. One possible direction is to concentrate on fitting probability distributions along the ideas of non-parametric density estimation, Silverman [17]. Experience with remote sensing data by Rijal and Noor [1] suggests that density estimation techniques are difficult. Instead the authors are currently considering wavelet representation of line profiles of selected parts of the images. For a given area on the X-ray films identified positively by the medical practitioner as being infected by tubercle bacilli, a series of line profiles (using MATLAB software, see Misiti *et al.* [18]) and its corresponding Daubechies Wavelet representation were obtained. The line profiles were of equal length and chosen vertically between ribs in the confirmed affected area. This is to ensure that the same number of Daubechies Wavelet detail coefficients were obtained for each line profile.

A given patient was selected and we now investigate whether the coefficients (represented as vectors) are identical or 'similar'. If many lines profiles exhibit identical or 'similar' vectors of coefficients we may say that these coefficients is typical (possibly represent) of the disease MTB, and hence may be used as an indicator of MTB. Current work involves applying clustering technique, see Everitt [19].

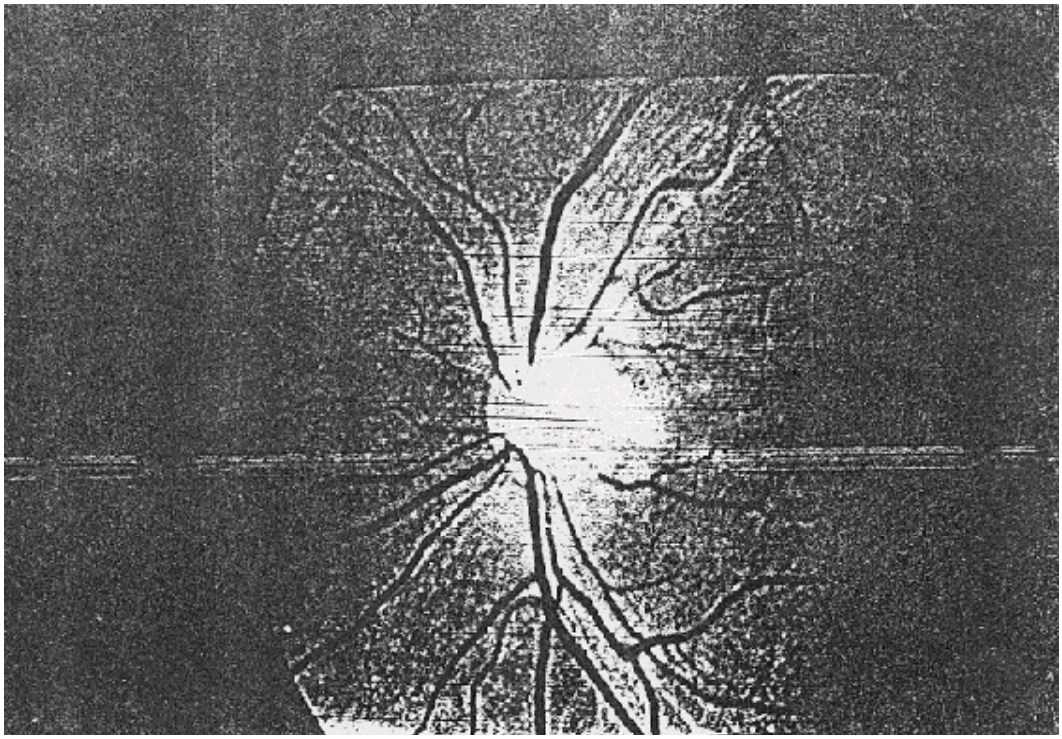

Figure 4 Image of the Eye Retina

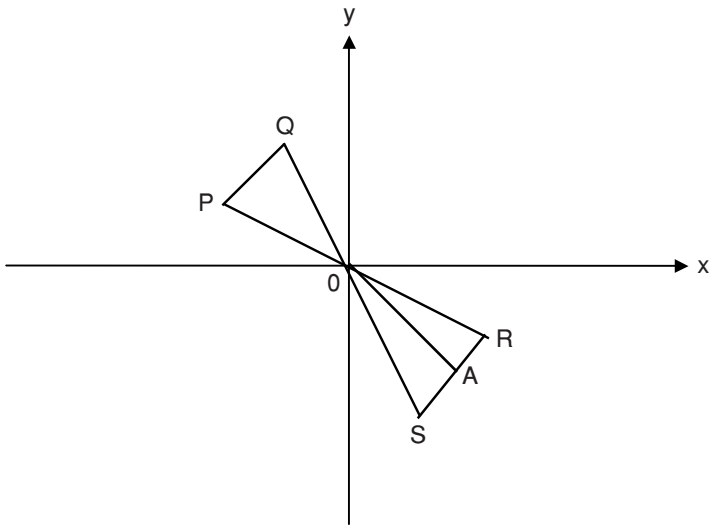

Figure 5 The Wedge Filter. The Filter Parameters are; (i) Φ = Angle AOB. (ii) C = Angle POQ = Angle SOR (i.e. opening of the wedge), and (iii) r = radius = OA

Example 2: Glaucoma

Glaucoma is a disease that involves the death of nerve fibers in the eye. Early detection is essential to enable treatment to be effectively applied; otherwise blindness results. In this study, the picture of the eye retina received from medical centre is scanned into an image processing workstation. Figure 4 shows the eye retina; the lines in black are the arteries and the white lines are the minute nerves. The task here is to discriminate between dead nerves and 'non-dead' nerves.

The 'wedge filter' will be used to enhance the image. Figure 5 is an illustration of a wedge filter where the three parameters Φ, C and r could be selected so that the filter may have properties resembling a combination of the ideal low pass filter (ILPF) and that of the ideal high pass filter (IHPF). For ease of calculations, the Fast Fourier transforms will be used to calculate the Fourier transforms and its inverse.

The first step is to obtain the logarithms of $f(x,y)$, say $F(x,y) = \ln [f(x,y)]$. Next we obtain the Fourier transform of $F(x,y)$ say $G(u,v)$; see Gonzalez and Wintz [20]. Finally we multiply $G(u,v)$ with the filter $H(u,v)$. A pictorial representation of the wedge filter is illustrated in Figure 5. In the frequency domain (i.e. the (u,v) space) the values of $H(u,v)$ equals one for values of (u,v) within Δ PQO and Δ SOR as shown in Figure 5; and takes the value zero elsewhere. We may denote $H(u,v)$ as follows;

$$\text{let} \quad \delta(u,v) = \begin{cases} 0 \text{ if } (u,v \in [\Delta PQO \text{ or } \Delta SOR) \\ 1 \text{ if } (u, v) \text{ in other areas} \end{cases}$$

$$\text{and} \quad H(u,v) = 1 - \delta(u,v)$$

It should be noted is that all transformations involved here are one-to-one. In particular the Fourier transform $G(u,v)$ is a one-to-one transform of $F(x,y)$; see Rudin [21] and Apostol [22].

In other words, we get a unique inverse for the transformed image. Computationally, the discrete inverse Fast Fourier transform is used to obtain the 'filtered' $F(x,y)$, viz;

$$f^*(x,y) = \frac{1}{N} \sum_u \sum_v GH(u,v) \exp[{}^{-j2\pi(ux+vy)}/_{N}]$$

where $GH(u,v) = G(u,v)H(u,v)$ and $j = \sqrt{-1}$. The final step is of course to take the exponent of $f^*(x,y)$.

The experiment involves varying the size and orientation of the wedge filter. Parameter Φ gives the orientation of the wedge filter and is taken from 0° to 180° at 10° increment. Parameter C and r gives the size of the wedge filter. Parameter r is given the value 100 so that more of the high frequency components will be selected. Parameter C which is the opening of the wedge filter is chosen to have values between 5° to 90°. For each selected combination of C, Φ and r, an expert looked at the filtered

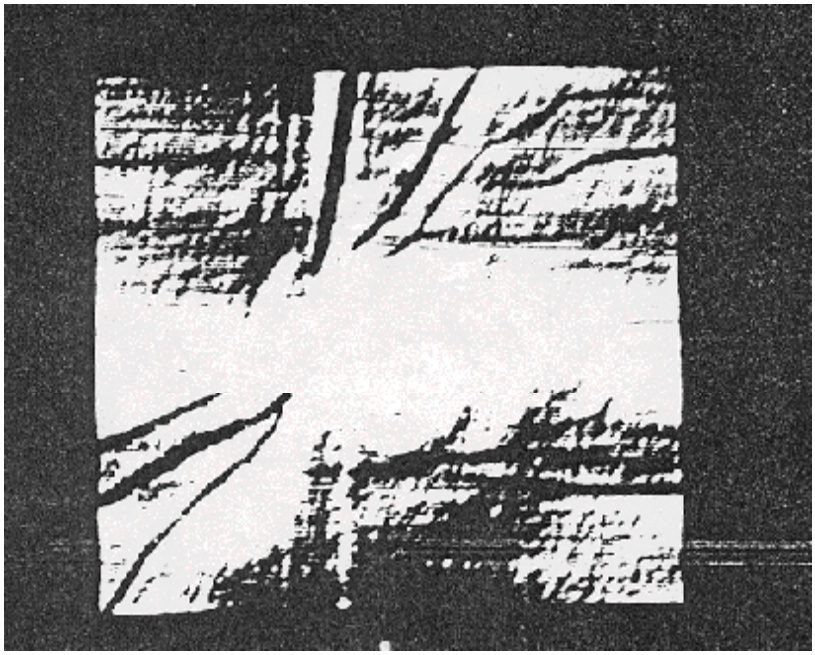

Figure 6 The Resultant Image Inverted Transform of the Eye Retina after Applying the Wedge Filter with C = 15°, Φ = 90° and r = 100

image. The 'best' image selected by the expert correspond to the parameter values of $C = 15°$, $\Phi = 90°$ and $r = 100$.

It is not obvious here (for the same patient) that a comparison of two images (before or after medication) would enable a statistical study similar to that of Example 1. This is most likely due to the problem of having to detect 'fine' nerves. This would suggest the need for more complicated image modeling. Experimental results from Cross and Jain [5] suggest that an image of a set of fine lines may possibly be modeled by the binomial random field texture model. Figure 6 of Cross and Jain [5] suggest that modeling the fine lines is equivalent to modeling anisotopic line textures.

Example 3: Recognition Of Symbols In Utility Maps

In this example, a procedure is developed for the efficient entry of design drawings or maps into the computer. In particular, the automatic recognition of plant symbols on utility maps is desired, see Manaf et. al. [23]. This study involves 3 stages namely

(a) preprocessing and feature extraction (segment list)
(b) matching procedure
(c) classification procedure

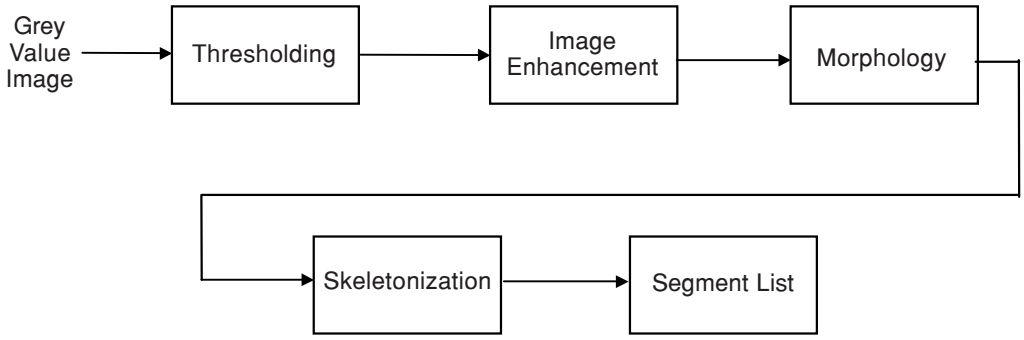

Figure 7 Procedure for Obtaining a Segment List

Obtaining Segment Lists

Utility symbols are scanned with a Mikrotech Scanner connected to a Macintosh and stored in raster format. The different symbols are stored in individual files and these images are then preprocessed by the procedure illustrated in Figure 7. Image enhancement requires the scanned image to be threshold, filtered, morphologised and skeletonized to ensure that the 'best image' is obtained for further matching and classification purposes. This image is then converted into a segment list.

A segment list can be thought of as a vector of line that makes up a utility symbol. Twenty symbols are converted into segment lists and are called prototypes. One of these symbols is then chosen at random, scanned and converted to a segment list (test image) and is matched with the segment lists of the twenty prototypes. The whole procedure of Figure 7 was implemented by SCIL_Image [24], an image processing software that resides on a SUN-4 workstation running on a UNIX operating system.

Matching

For each line segment of the test image, a searching rectangle is defined (following Bart and Duin [25]) whose length and width are defined as

$$w_z * /\cos(\phi_i)/ * L_i \tag{1}$$

$$w_z * /\sin(\phi_i)/ * L_i \tag{2}$$

L_i is the length of the test segment, ϕ_i is its angle with the x-axis, and w_z is the weight coefficient for the searching rectangle. For minimum searching rectangles, the length and width of the searching rectangle is as follows:

In the x-direction:

$$w_z * /\cos(\phi_i)/ * L_i \quad \text{if} \quad w_z * /\cos(\phi_i) > w_{z\,\lim} \tag{3}$$

$$w_{z\,\lim} * L_i \quad \text{if} \quad w_z * /\cos(\phi_i)/ \leq w_{z\,\lim} \tag{4}$$

In the *y*-direction:

$$w_z * /\sin(\phi_i)/ * L_i \quad \text{if} \quad w_z * /\sin(\phi_i)/ > w_{z\,\lim} \tag{5}$$

$$w_{z\,\lim} * L_i \quad \text{if} \quad w_z * /\sin(\phi_i)/ \leq w_{z\,\lim} \tag{6}$$

where $w_{z\,\lim}$ is the weight coefficient of the minimum searching rectangle if the angle of the test segment tends to 0° or 90° with respect to the *x*-axis. In particular, a segment from the test image is considered matched to a given segment of the prototype image if:-

(i) The midpoint of the prototype segment lies in the searching rectangle.
(ii) The angle difference is less than a certain threshold.
(iii) The ratio of the length of the prototype segment and the test segment is within a predefined value.

In addition to the above conditions used by Bart and Duin [25], we also included the gradient of the segment as an additional criterion.

A Classification Procedure

Denote $T(i)$ as the i^{th} line segment for the test image and $P(j,k)$ as the j^{th} line segment for the k^{th} prototype where $i = 1, 2, ..., I$ and $j = 1, 2, ..., J$ and $k = 1, 2, ..., K$. We denote I as being the size of the segment list of the test image T, while J being the size of the segment list of the prototype P and K is the number of prototypes.

Cost Function $C[T(i), P(j,k)]$

The cost of matching $T(i)$ with a corresponding segment of prototype $P(j,k)$ is given as follows:

$$C[T(i), P(j,k)] = (W_L * \Delta L) + (W_\phi * \Delta\phi) + (W_X * \Delta X) + (W_Y * \Delta Y) \tag{7}$$

where ΔL, $\Delta\phi$, ΔX, ΔY is the difference in length, angle, *x* coordinate of midpoint, *y* coordinate of midpoint of the test segment and prototype segment respectively.

The Euclidean Distance

Firstly, we create a vector of minimum cost between a test image say $T(.)$ and a prototype (say $P(.,1)$). We calculate the minimum cost C_1 for the first segment of the test image as:

C_1 = min cost for matching $[T(1), P(j,1)]$, j = 1, 2, ..., J where J is the size of the segment list of the first prototype.

We repeat until C_I = min cost for matching $[T(I), P(j,1)$, j = 1, 2, ..., J where I is the size of the segment list of the test image. We thus obtain a vector of minimum costs of T and the first prototype as $(C_1, C_2, ..., C_I)$. Henceforth, the Euclidean distance between $T(.)$ and the first prototype is defined as:

$$d[T,P(.,1)] = \text{SQRT } (C_1^2 + C_2^2 + ... + C_I^2)$$

We then calculate the distance of the test image with $(k - 1)$ other prototypes as shown below

$$d[T, P(.,k)], \quad k = 2, 3, ..., K$$

and if min $d[T, P(.,k)] = d[T, P(.,k^*)]$, then we say that the test image T has been matched with prototype k^*.

Some Results

We have a 20% error rate that is largely due to symbols that are similar (see Figure 8(a) and 8(b)). Due to noise during preprocessing, the number of segments produced by the test image differs to that of the prototype of the same type. Ideally, unmatched segments are assigned to maximum costs. In practice, extra segments from prototypes of similar symbols do not give any contribution to maximum costs because all segments from the unknown test image is already matched to segments of the similar

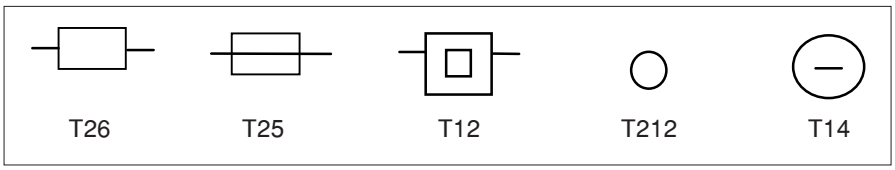

(a)

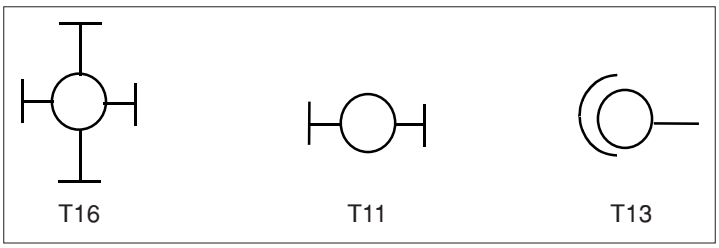

(b)

Figure 8 Examples of (a) Similar Symbols and (b) Non-Similar Symbols

symbols of the prototype and this leads to misclassification. Entirely different symbols do not give rise to these problems at all.

The above results may be improved if we repeat the above experiment in a more general or wider application. Specifically when a very large number of symbols need to be considered, plus the fact that symbols may originate from more than one 'company' or 'institution', we need to simultaneously apply several clustering techniques. Mardia, Kent and Bibby [26] remarks that applying and comparing the results of several different techniques help to prevent misleading solutions being accepted. Everitt [19] and Jardine and Sibson [27] give a discussion of this problem.

3.0 DISCUSSION

From the above examples, and that given in Rijal and Noor [2], the following points are noted.

Issue 1 : Different imagery requires different methods of analysis. The approach adopted usually is application or goal oriented.
Issue 2 : Enhancement and restoration techniques may be described as qualitative techniques. Historically, they dominate the analysis of images. Quantitative techniques are more recent. This suggests the complicated nature of mathematically modeling images.
Issue 3 : Image analysis should be a multi-disciplinary field.
Issue 4 : A measure of the quality of inference is seldom considered. Just how 'good' is our conclusion?

It is well known that these 'issues' effect the quality of inference or conclusion and what is crucial is how may statistical methodology help. For a given problem and a given image, statistical methodology may suggest a suitable 'descriptor' or 'statistic' to help solve the particular problem. Occasionally image problems may also be solved if the whole image can be modeled probabilistically.

In the MTB example where economic considerations force the use of cost-effective scanner to produce a digital X-ray image; decisions based on low quality images have to be made. The image histogram when used under consistent conditions, yield reliable comparison over two time points. Unfortunately, this result is useful only if the MTB patient has been identified earlier. Towards this purpose, the authors are considering wavelet representation of time profiles of selected parts of the image. Establishing the unique wavelet coefficients to identify MTB would then reduce a considerable amount of uncertainty mentioned in the introduction section.

For the example on Glaucoma, if observers can agree on a common set of filter parameters, the binomial Markov random field model may be consider an objective tool for the detection of the dead nerve.

In the final example, the image is well defined. Unfortunately, it is not obvious how we may define or calculate a statistic to 'represent' the symbols. However by applying other clustering techniques, such as the Nearest Neighbour method (Cover and Hart [28]), the recognition of symbols may be improved.

The remote sensing example of Rijal and Noor [2] is an illustration of the case where image analysis should be a multidisciplinary field. The manpower needed involves are the computer scientist, communication engineer, and ideally he mathematician or statistician. In practice, however, it is often the case that the communication engineer would perform an image analysis using some software; and may only occasionally consult the mathematician or statistician on specific aspects of the image analysis. Nevertheless, this example is a case where statistical modeling and inference can be applied.

Issue 4 is a problem with all the examples. When image models are available, misclassification probabilities may be defined when we compare two images (the original image and the processed image). Nevertheless, there are some conceptual problems with the definition of misclassification probabilities, see for example Lachenbruch [29]. However, on a practical note, measuring the quality of inference based on image models are to be preferred to non-probabilistic models, whenever possible.

4.0 CONCLUSION

Statistical methodology may be applied on any digital image to produce information descriptors or statistics or occasionally an image model that may help to provide solutions to a given problem. In situations when the limitations of a given technology is exceeded (for example increasing the capabilities or optimal output of a given set of equipment is no longer possible), useful information may still be derived from the experimental data by a judicious application of statistical methodology.

REFERENCE

[1] Rijal, O. M. and N. M. Noor. 1995. On Statistical Image Segmentation For Remotely Sensed Data. *Jurnal ELEKTRIKA*, Jilid 8, Bil. 2, Universiti Teknologi Malaysia publication. 59–72.

[2] Rijal, O. M. and N. M. Noor. 1998. Uncertainty in Digital Image Analysis. *ELEKTRIKA*, *Journal of electrical Engineering*. 1(1): 16–22.

[3] Besag, J. E. 1974. Spatial Interaction And The Statistical Analysis Of Lattice Systems. *Journal of Royal Statistical Society (B)*. 192–236.

[4] Besag, J. E. 1972. Nearest Neighbor Systems And The Auto-logistic model for binary data. *Journal of Royal Statistical Society (B)*. 34: 75–83.

[5] Cross, G. R. and A. K. Jain. 1983. Markov Random Field Texture Models. *IEEE Trans. On Pattern Analysis And Machine Intelligence*. PAMI-5(1): 25–39.

[6] Ripley, D. 1986. Statistics, Images And Pattern Recognition. *The Canadian Journal of Statistics*. 14(2): 83–111.

[7] Derin, H. and H. Elliot. 1987. Modelling And Segmentation Of Noisy And Textured Images Using Gibbs Random Fields. *IEEE Trans. On Pattern Analysis And Machine Intelligence*. PAMI-9: 39–55.

[8] Samadani, R. 1995. A Finite Mixtures Algorithm For Finding Proportions In SAR Images. *IEEE Trans. On Image Processing*. 4(8): 1182–1186.
[9] Noor, N. M., O. M. Rijal, O. M. Badar and Y. T. P'ng. 2001. A Mixture Distribution For The Wire Bonding Image. *Proceedings of the 6th International Symposium On Signal Processing And Its Applications (ISSPA 2001)*. 2: 655–657.
[10] Sclove, S. C. 1983. Application Of The Conditional Population Mixture Model To Image Segmentation. *IEEE Trans. Pattern Analysis And Machine Intelligence*. PAMI-5: 428–433.
[11] Duin, R. P. W. 1976. On The Choice Of Smoothing Parameters For Parzen Estimators Of Probability Density Functions. *IEEE Trans. On Computers*. 1175.
[12] Haralick, R. M. and K. Sam Shanmugam. 1974. Combined Spectral And Spatial Processing Of ERTS Imagery Data. *Remote Sensing Of Environment*. 1: 3–13.
[13] Haralick, R. M., K. Sam Shanmugam and I. Dinstein. 1973. Textural Features For image Classification. *IEEE Trans. On Systems, Man and Cybernetics*. SMC-3(6): 610–621.
[14] Middlemiss, H. 1982. Radiology of the future in developing countries. *British Journal of Radiology*. 55: 698–699.
[15] Moores, B. M. 1987. Digital X-ray Imaging. *IEE Proceedings*. Vol. 134 Part A (2). Special Issues On Medical Imaging.
[16] Toman, K. 1979. *Tuberculosis: Case Finding And Chemotherapy*. W.H.O. Report, 28.
[17] Silverman, B. W. 1986. *Density Estimation for Statistics and Data Analysis*. Chapman and Hall. 113–124.
[18] Misiti, M., Y. Misiti, G. Oppenheim, and J-M. Poggi. 1996. *Wavelet Toolbox For use with MATLAB*. 1.15–1.34.
[19] Everitt, B. S. 1977. *Cluster Analysis*. London: Heinemann Educational Books Ltd.
[20] Gonzalez, R. C. and P. Wintz. 1977. *Digital Image Processing*, Addison-Wesley. 36-112 and 166–169.
[21] Rudin, W. 1973. *Functional Analysis*. Mac-Graw-Hill.
[22] Apostol, T.M. 1974. *Mathematical Analysis*. Addison-Wesley.
[23] Manaf, A. A., O. M. Rijal, and G. Sulong. 1994. Automatic Recognition of Symbols in Utility Maps, *The Proceedings of IEEE TENCON 1994*. Singapore. 857–861.
[24] SCIL Image, Manual, University of Amsterdam, For Centre Of Image Processing And Pattern Recognition.
[25] Bart, M., and R. P. W. Duin. 1990. *Technical Report On Recognition Of 3-D Objects From 2-D Images Based On A Learning Set Of Images*. University of Amsterdam.
[26] Mardia, K. V., J. T. Kent, and J. M. Bibby. 1979. *Multivariate Analysis*. Academic Press. 384–385.
[27] Jardine, N., and R. Sibson. 1971. *Mathematical Taxonomy*. New York: Wiley.
[28] Cover, T. M., and P. E. Hart. 1967. Nearest Neighbor Pattern Classification, *IEEE Trans. Information Theory*. 13(1): 21–27.
[29] Lachenbruch, P. A. 1975. *Discriminant Analysis*. Hafner Press. 29–36.